Electric Power Systems Research 166 (2019) 73–82

Contents lists available at ScienceDirect

Electric Power Systems Research

journal homepage: www.elsevier.com/locate/epsr

# Reliability assessment method of composite power system with wind farms and its application in capacity credit evaluation of wind farms

Fan Chen[a,*], Fangxing Li[b], Wei Feng[b], Zhinong Wei[c], Hantao Cui[b], Haitao Liu[a]

[a] School of Electric Power Engineering, Nanjing Institute of Technology, Nanjing 211167, China
[b] Dept. of EECS, The University of Tennessee, Knoxville, TN 37996, USA
[c] College of Energy and Electrical Engineering, Hohai University, Nanjing 210098, China

ARTICLE INFO

*Keywords:*
Composite power system reliability
Wind farms
Non-sequential Monte Carlo Simulation
State merging
Parallel computing
Capacity credit

ABSTRACT

This paper presents a non-sequential Monte Carlo Simulation (MCS)-based method for the reliability assessment of composite power system with wind farms (WFs). A multistate probability table and its corresponding Spearman's rank correlation coefficient (SRCC) are combined to represent the power outputs of WFs, which makes the multistate model of WFs compatible with the non-sequential MCS while considering the dependence among power outputs of WFs. By constructing a system state array with encoding conversion, a state merging technique is proposed, which significantly reduces the number of system states to be evaluated. In addition, the parallel computing technique is employed to accelerate the contingency analysis for the merged system states. Furthermore, the capacity credit (CC) of WFs considering both wind power correlation and transmission network constraints is evaluated based on the proposed reliability assessment method. Finally, the effectiveness of the proposed reliability assessment method and its application in the CC evaluation are demonstrated using extensive numerical studies on several modified test systems.

## 1. Introduction

Composite power system reliability is concerned with the problem of assessing the ability of generation and transmission system to supply adequate electrical energy to the major load points [1]. It has been successfully applied in many areas, such as generation source planning, transmission development planning, transmission operation planning and operating reserve assessment [2,3]. Meanwhile, in recent years, wind power generation has been rapidly and widely developed worldwide for tackling the problems of environmental pollution and energy supply sustainability. Due to the intermittent and variable nature of wind speed, output power of wind farms is stochastic and quite different from those of conventional units. Thus, there is a pressing need for studying the reliability evaluation of composite power system with wind power integration.

The composite power system reliability evaluation generally involves three basic steps: selecting system states, evaluating the consequences of selected system states and calculating risk indices [2]. Analytical enumeration and Monte Carlo Simulation (MCS) are two primary approaches that have been proposed to select system states. Though the analytical method can obtain the exact reliability indices by explicitly or implicitly identifying all possible system states, it is rarely used in reliability assessment of composite power system with wind farms (WFs). The reason is that analytical method has difficulty in assessing reliability for practical-size systems due to the curse of dimensionality [3], as well as difficulty in building analytical models of WFs considering wind power correlation. Naturally, it is sensible to use MCS for reliability assessment of composite power system with WFs. The MCS can be further categorized into sequential and non-sequential simulation. The sequential simulation moves chronologically through the system states, while the non-sequential simulation selects the system states randomly [4]. In the past few decades, researchers have conducted considerable studies on the improvement of MCS for power system reliability. To take advantages of the computational efficiency of non-sequential MCS and the accuracy of sequential/chronological simulation, pseudo-sequential and pseudo-chronological MCS were proposed in Refs. [5,6] for calculating the loss of load cost (LOLC), respectively. In Ref. [4], quasi-sequential MCS was proposed in order to deal with time-dependent aspects such as load variation, generating capacity fluctuation from renewable sources, and maintenance. Aiming at improving the computational efficiency of MCS, kinds of variance reduction techniques, such as importance sampling [7], Latin hypercube sampling (LHS) [8], cross-entropy methods [9] and subset simulation [10] were proposed in recent years. From the perspective of

* Corresponding author.
*E-mail address:* fanchen_nj@163.com (F. Chen).

https://doi.org/10.1016/j.epsr.2018.09.023
Received 15 April 2018; Received in revised form 12 August 2018; Accepted 30 September 2018

evaluation process of power system reliability, these variance reduction techniques can be summarized as accelerating computation at the first stage of system reliability assessment, i.e., selecting system states. Based on this perception, we were inspired to accelerate computation of composite power system reliability at another stage of evaluation process. In this paper, an accelerating method based on non-sequential MCS is proposed to deal with the sampled system states. The proposed method is based on the observation that a large number of system states sampled by non-sequential MCS are repetitive. Thus, if we can avoid conducting contingency analysis for the repeating system states, the computation effort will be greatly reduced. In this paper, we skillfully merge all of the sampled system states by constructing system state arrays with encoding conversion technique. The main contributions of this paper can be summarized as follows:

(1) A multistate probability table and its corresponding Spearman's rank correlation coefficient (SRCC) are combined to represent the probabilistic characteristics of WFs power outputs, allowing the consideration of wind power correlation under the framework of non-sequential MCS.
(2) Several innovative techniques are utilized to speed up the analysis for thousands of simulated system states. First, the binary array with respect to a system state is constructed and represented by a decimal number. This makes it convenient to identify and merge system states obtained by non-sequential MCS, and thus greatly reduces the number of system states under analysis. Second, the parallel computing technique is used for contingency analysis of the merged system states, which accelerates the process of state evaluation significantly.
(3) On the basis of the proposed reliability evaluation method of composite power system with WFs, capacity credit (CC) evaluation of WFs considering both wind power correlation and transmission constraints is implemented. This is different from existing literatures which only consider wind power outputs correlation or transmission constraints [11–13].

The remainder of this paper is organized as follows. Section 2 presents the non-sequential MCS-based reliability evaluation method of composite power system with dependent WFs. Section 3 shows the application of the proposed reliability evaluation method in the CC evaluation of WFs considering both wind power correlation and transmission constraints. The effectiveness of the proposed reliability evaluation method and the necessity of incorporating both wind power correlation and transmission constraints in the CC evaluation are verified by a number of numerical tests in Section 4. Finally, conclusions are made in Section 5.

## 2. Fast reliability evaluation method of composite power system with WFs based on non-sequential MCS

Three aspects of the work have been completed to develop an efficient non-sequential MCS-based method for evaluating the reliability of composite power system with WFs in this section: the state sampling of independent conventional generation units, lines and dependent WFs outputs, the reduction of number of system states to be evaluated and the parallel computing of merged system states. The implementation of these three contributions is demonstrated as follows.

### 2.1. Components state sampling of composite power system with WFs

The non-sequential MCS method is also called the state sampling approach, and it is based on the fact that a system state is a combination of all component states. In order to evaluate reliability of the composite power system with WFs using a non-sequential MCS, the states of conventional generating units, transmission lines and WFs have to be determined first. Generally, the conventional generating units and transmission lines are assumed to have two states of failure and success. Their failures are independent of each other [2]. In this context, each component state of generating units and transmission lines can be modeled by producing random numbers distributed uniformly between [0,1]. Let $PF_i$ denote the $i$th component failure probability and $U_i$ denote a random number distributed uniformly between [0,1]. Then the state of the $i$th component $S_i$ can be determined by:

$$S_i = \begin{cases} 1\ (failure), & 0 \le U_i < PF_i \\ 0\ (success), & PF_i \le U_i \le 1 \end{cases} \quad (1)$$

In order to adapt to the non-sequential MCS, a wind farm is supposed to be represented as a generating unit with multistate output power [14]. The multistate probability table [15,16] of a wind farm is generally constructed and used to sample the output power state of a wind farm. In Ref. [17], the sequential output power series of a WF considering both wind speed correlation and wind turbine generator (WTG) outage was developed by using a Copula function. Subsequently, the multistate model of the total wind power generation system was built by using an apportioning technique. Additionally, this multistate output power model has been used for reliability evaluation of generating system with WFs. However, when it comes to the reliability evaluation of composite power system with farms, there are two issues needing to be addressed. First, the multistate probability table of each wind farm, instead of the probability table of wind power of all WFs, has to be modeled for composite system reliability, as WFs are generally integrated into power system at different buses. Fortunately, similar to modeling the multistate probability table of all of the WFs [17], this issue is easy to be solved by applying an apportioning technique to the simulated output power series of each WF. Second, it should be noted that there exists correlation between power outputs of WFs in adjacent areas [18], and thus the state sampling of each WF cannot be determined by using independent random numbers, which is quite different from the state sampling of conventional system components. Pearson correlation and rank correlation are two coefficients used to measure the dependence among random variables in power system analysis. Compared with rank correlation coefficient, Pearson correlation coefficient is not invariant under non-linear strictly increasing transformations in cases of non-normally distributed variables [19,20]. And on the other hand, it is pointed out in Refs. [19,21] that the WF power output does not follow the Normal distribution, thus it is wise to choose rank correlation to measure the dependence among WFs power outputs. Rank correlation coefficients, including Spearman's rank correlation coefficient, Kendall's rank correlation coefficient and Gini correlation coefficient, are mainly used to measure the degree of monotonic dependence between random variables [18,22]. Considering that the Spearman correlation between two variables is equal to the Pearson correlation between the rank values of those two variables [23], we are inspired to use correlated random variables following uniform distribution between [0,1] to simulate dependent WFs outputs. In this paper, the procedure of sampling correlated WFs outputs compatible with a non-sequential MCS is proposed as follows:

(1) Simulate sequential output power series of WFs considering wind speed correlation, WTG outage, and dependency between WTG outage and wind speed. The detailed process was shown in [17].
(2) Calculate the Spearman correlation coefficient $R_p$ between WFs power outputs based on the sequential wind power series generated in Step (1).
(3) Use apportioning technique to create multistate probability table of WFs from sequential wind power series generated in Step (1).
(4) Produce random numbers distributed uniformly between [0,1] with specified linear correlation coefficient $R_p$. This step is convenient to implement by Copula method.
(5) Determine WF output states according to the random numbers generated in Step (4). Assume that $X_i$ is a random number generated

in Step (4), then the output state of the $i$th wind farm can be determined by:

$$s_i = \begin{cases} 0,\ 0 \le X_i < p_{WFi(1)} \\ 1,\ p_{WFi(1)} \le X_i < (p_{WFi(1)} + p_{WFi(2)}) \\ \vdots \\ k,\ \sum_{j=1}^{k} p_{WFi(j)} \le X_i < \sum_{j=1}^{k+1} p_{WFi(j)} \\ \vdots \\ n_{eq} - 1,\ \sum_{j=1}^{n_{eq}-1} p_{WFi(j)} \le X_i \le 1 \end{cases} \quad (2)$$

where $s_i$ denotes the state number of the $i$th wind farm; $n_{eq}$ is the total number of WF equivalent states; and $p_{WFi(j)}$ is the $j$th state probability of the $i$th wind farm.

### 2.2. Contingency analysis for sampled system states based on state merging and parallel computing techniques

#### 2.2.1. Construction of binary array of a system state

For a simulated system state including states of conventional generating units, transmission lines and WF outputs, system state analysis needs to be conducted to provide a load curtailment value for updating system reliability indices. The system state analysis is a complicated and computationally expensive problem associated with power flow, contingency analysis and remedial actions. In this paper, a technique based on constructing system state arrays is proposed for identifying and merging the sampled system states. By merging the repeating system states, the number of system states to be evaluated reduces dramatically.

As mentioned in the previous section, a conventional generating unit or transmission line is usually represented as a two-state component, and a WF is generally modeled as a multistate generating unit. Consequently, the system state can be determined by combing the states of all components. In this paper, the state array composed of 0 or 1 element is proposed to represent the system operation status. The system state array is constructed like this: for a two-state component (i.e., conventional generating unit or transmission line), one array element is used to represent its operation state; for a multistate WF, several array elements are used to represent its output. For example, if a WF is equivalent to a generating unit with $n_{eq}$ states, then the operation state of WF can be represented by $n_w$ array elements. The $n_w$ is determined by:

$$n_w = \text{ceil}(\log_2 n_{eq}) \quad (3)$$

where the function ceil(x) represents rounding up x to the nearest greater integer.

By storing a single binary number representing the state of a transmission line or a generating unit and a string of binary numbers representing the state of a WF in an array successively, a specified system state array can be constructed. Assume that a composite system consists of $nl$ transmission lines, $ng$ generating units and $n_{WF}$ WFs, then a binary system state array is comprised of elements as follows:

(1) The first $nl$ elements in the state array represent the states of $nl$ transmission lines: "1" represents that a transmission line is in service, while "0" represents that a transmission line is out of service.
(2) The following $ng$ elements in the state array represent the states of $ng$ generating units: "1" represents that a generating unit is in service, while "0" represents that a generating unit is out of service.
(3) Assume that each WF output state is represented by $n_w$ binary numbers. Then the last $n_w \times n_{WF}$ elements in the state array represent the states of $n_{WF}$ WFs. The value of $n_w$ is dependent on the equivalent number of WF states. For example, if a WF is supposed to be modeled as a generating unit with 11 output states, then 4 binary numbers are used to represent the WF output state (i.e., $n_w = 4$). Considering that a WF is sampled to be in the "k" status according to Eq. (2), we convert the decimal number $k$ into $n_w$ binary numbers and then fill these $n_w$ binary numbers into the system state array. To illustrate the binary representing method of a WF, we assume that a WF has 11 equivalent output states. If the WF is sampled to be in the "0" status, then we use "0,0,0,0" to represent the state of this WF; if the WF is sampled to be in the "2" status, then we use "0,0,1,0" to represent the state of this WF.

| Components | $L_1$ | … | $L_{nl}$ | $G_1$ | … | $G_{ng}$ | $WF_1$ | | | | …… | $WF_{n_{WF}}$ | | | |
|---|---|---|---|---|---|---|---|---|---|---|---|---|---|---|---|
| Binary code | 1 | … | 1 | 0 | … | 1 | 1 | 0 | 0 | 1 | …… | 1 | 1 | 0 | 1 |

**Fig. 1.** The binary array representing a system state.

A typical binary array representing a system state is shown in Fig. 1, where L denotes transmission lines, G denotes generating units, and WF denotes wind farms.

#### 2.2.2. Process of identifying and merging system states

By representing the system states sampled by a non-sequential MCS with binary arrays, the identification between system states is transformed to be the criterion of comparisons between the state arrays. In this paper, the comparison between two state arrays is proposed to be implemented by an encoding conversion method.

The flowchart of sampling, identifying and merging system states based on non-sequential MCS is shown in Fig. 2. For a certain string of binary codes saved in the state array, it is converted to its equivalent decimal number to mark a system state. Then, this decimal number is searched in the history decimal numbers to check whether this system state has been previously sampled. If a decimal number marking a special system state can be found, this sampled system state is a repeated state and should be merged. To sum up, for a specific system state, the information needing to be saved includes the binary codes representing this system state, its equivalent decimal number and the number of occurrence times of this system state.

#### 2.2.3. Parallel computing on analyzing the merged system states

With the rapid development of computer and communication technologies, the parallel computing technique has been widely applied in many engineering problems, such as load flow analysis [24], power system security analysis [25] and optimum allocation of distributed generation units [26]. It is noted that the contingency analysis of system states are independent from each other. This implies that the state analyses are suited for parallel computing. Data parallelism and task parallelism are the two schemes used for parallel computing. In this paper, data parallelism is used for analysis of the merged system states, i.e., the merged system states are split into multiple state sets and each state set is expected to be processed by different workers using the same instruction. In this paper, the proposed work has been carried out in Matlab enviroment, with Matlab Parallel Computing Toolbox Software (PCTS) used to implement parallel computing. The PCTS divides the system states analysis into various tasks and assigns different tasks to various workers of a multi-core computer.

Assume that the total number of system sampling states is $NS$, the number of merged system states is $Nm$ and the number of computing resources is $l$. Then the anaysis for the $Nm$ system states are evenly distributed to $l$ computing resources. The flow chart of system states analysis using parallel computing is shown in Fig. 3.

### 2.3. Calculation of reliability indices

As shown in Fig. 3, the load curtailments of $Nm$ system states are concurrently computed by multiple processors. By collecting the load

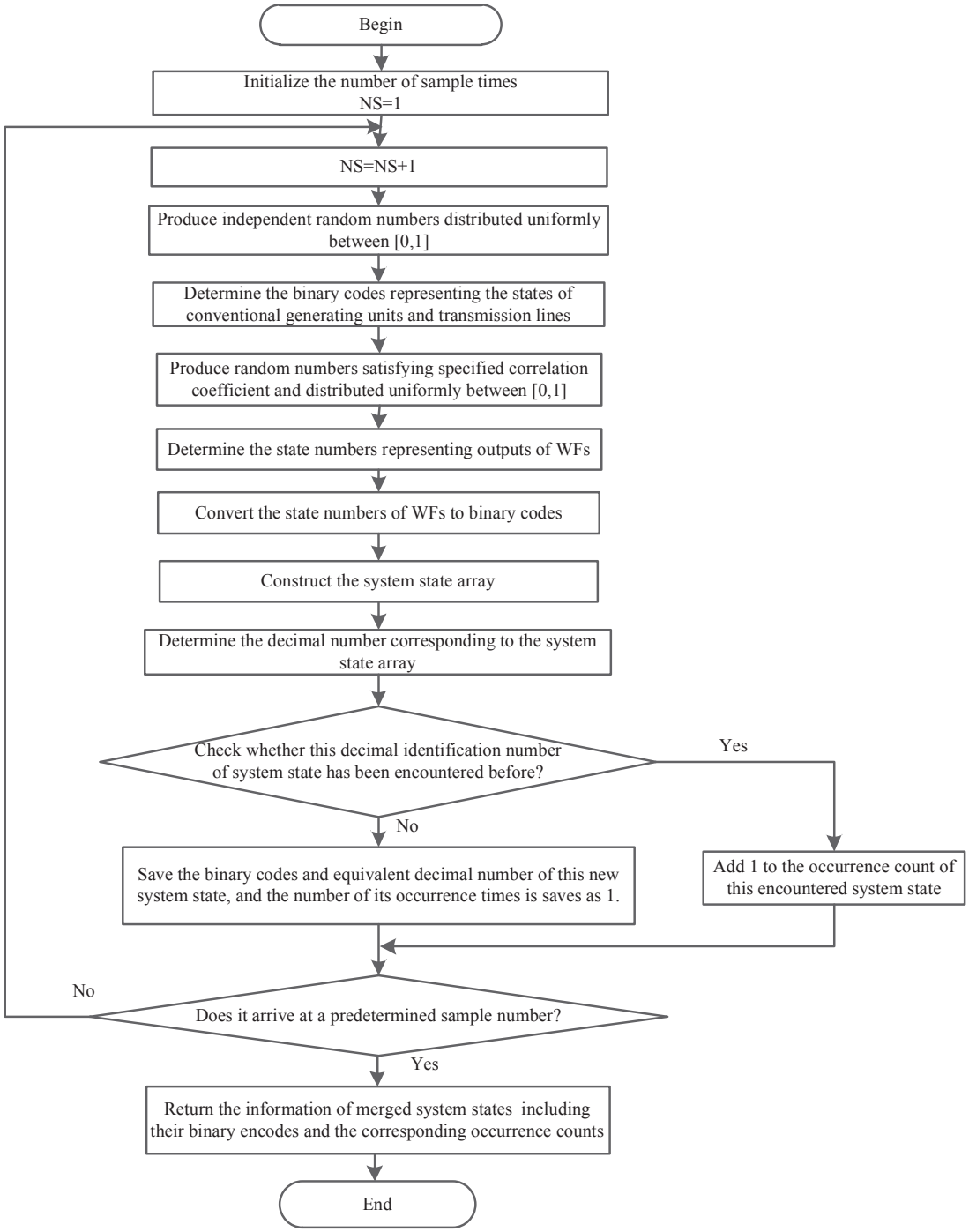


**Fig. 2.** Flowchart of sampling, identifying and merging system states based on non-sequential MCS.

curtailments returned by all of the parallel processors, the reliability indices can be obtained. Probability of load curtailments (PLC) and expected energy not supplied (EENS) are two commonly used reliability indices, and in this paper they are formulated as follows:

$$PLC = \sum_{i=1}^{Nm} \left( I_i \times \frac{ns_i}{NS} \right) \tag{4}$$

$$EENS = \sum_{i=1}^{Nm} \left( CS_i \times \frac{ns_i}{NS} \times 8760 \right) \tag{5}$$

where $NS$ is the total number of system sampling states; $Nm$ is the number of system states after being merged; $ns_i$ is the number of occurrence times of the $i$th system state; $CS_i$ is the load curtailment of the $i$th system state; and $I_i$ is an indicator variable, which means:

$$I_i = \begin{cases} 0, & CS_i = 0 \\ 1, & CS_i \neq 0 \end{cases} \tag{6}$$

## 3. Capacity credit evaluation of WFs considering both wind power correlation and transmission constraints

As previously mentioned, the power output of WFs is highly uncertain due to the intermittent nature of wind speed. Therefore, it becomes an urgent issue for the utility company to evaluate to what extent the WFs could provide capacity contribution to power system when the

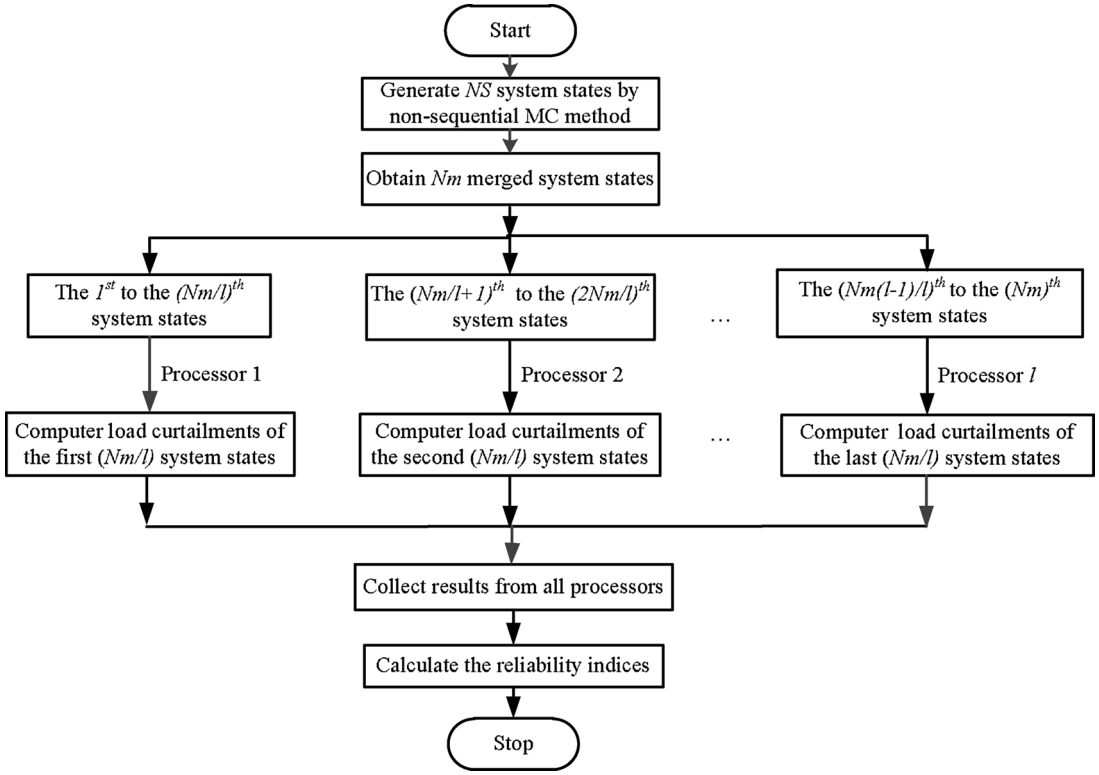


**Fig. 3.** Flow chart of system states analysis using parallel computing.

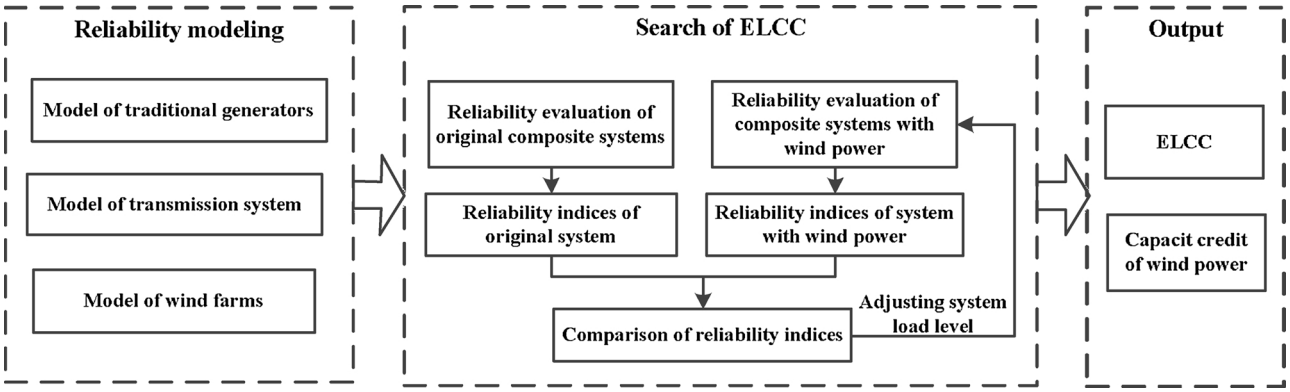


**Fig. 4.** The framework for the WFs CC evaluation.

long-term generation expansion planning is implemented. Generally, this problem is referred to as capacity credit (CC) evaluation of WFs. There exist several ways for defining CC in existing literature, and effective load carrying capability (ELCC) and equivalent firm capacity (EFC) are the two metrics most commonly used. ELCC is the amount of load that can be added to the system in the presence of wind generators while maintaining the system's reliability level, while EFC is the completely firm generating capacity which would give the same risk level if it replaces the wind power generation [11,12,27,28]. Some existing literatures have been conducted to investigate the CC of wind power. In Ref. [11], both the ELCC and EFC of WFs were evaluated by using a system well-being analysis approach at the generation level (hierarchical level I, HLI). In Ref. [12], a rigorous analytical model considering wind power correlation was derived; then the CC of wind power was also calculated at the generation level by a fast method based on the proposed analytical model. Unlike literature [11,12], in which the transmission constraint was ignored, the CC of wind power was evaluated at a composite system level (hierarchical level II, HLII) in Ref. [13]. Unfortunately, the wind speed correlation was not taken into consideration in Ref. [13]. As can be summarized from the literatures above, transmission constraints and wind power correlation are two factors affecting the CC of wind power. However, there is little literature considering both of these two factors. In this context, an assessment framework for the CC of WFs considering both transmission constraints and wind power correlation is presented, which is based on the proposed reliability evaluation method in Section 2. The ELCC approach is chosen to determine the CC of wind power in this paper based on the following considerations. When the EFC definition is employed, the CC of WFs depends on the location used to connect the equivalent firm generator to the composite power system, which makes it complicated to quantitatively study the effects of wind power correlation and transmission constraint. Whereas, when the ELCC definition is employed, it is convenient to quantitatively calculate the effective load under different cases, such as different wind power correlation or different network topology. The developed framework for the WFs CC evaluation, based on the reliability evaluation method presented in Section 2, is shown in Fig. 4.

## 4. Case studies

### 4.1. General setup

In order to validate the proposed reliability evaluation algorithm of composite power system integrated with WFs, and to demonstrate the necessity to consider both the correlation of power outputs of WFs and the transmission network constraints in the CC evaluation of WFs, two wind farms (WF_A and WF_B) are integrated into IEEE RTS 79 [29] to create five modified reliability test systems. For simplicity, it is assumed that each wind farm is composed of 100 identical wind turbine generators with a rated capacity of 2 MW and cut-in, rated, and cut-out speeds of 4, 10, and 22 m/s, respectively, and the forced outage rate (FOR) of each wind turbine generator is 0.05. Wind speeds of the two WFs follow Weibull distribution, and both have scaling and shape factor specified as 7.5 and 2.0, respectively. The five modified test systems used in this section are as follows:

- **MRTS_A1**: the two WFs are integrated into IEEE RTS 79 at buses 1 and 2, respectively.
- **MRTS_A2**: the FORs of conventional generating units of IEEE RTS 79 are reduced by half, and then the two WFs are integrated at buses 1 and 2, respectively.
- **MRTS_A3**: the capacity limits of all transmission lines of IEEE RTS 79 are reduced by half, and then the two WFs are integrated at buses 1 and 2, respectively.
- **MRTS_B1**: the two WFs are integrated into IEEE RTS 79 at buses 18 and 22, respectively.
- **MRTS_B2**: the capacity limits of all transmission lines of IEEE RTS 79 are reduced by half, and then the two WFs are integrated at buses 18 and 22, respectively.

In the analysis process for a specified system state, the load shedding policy aimed at minimizing the total load curtailment is used to reschedule generations and eliminate constraint violations. A series of numerical tests are performed on a dual-core, four-thread personal computer with Intel (R) Core(TM) i5-3427U CPU (1.8 GHz) and 4 GB RAM. Programs are executed in MATLAB.

### 4.2. Verification of the proposed reliability evaluation algorithm of composite power system with WFs

#### 4.2.1. Probabilistic models of WFs compatible with non-sequential MCS

As mentioned in Section 2, to be compatible with non-sequential MCS and to preserve the characteristics of wind power correlation, WFs are represented by combination of a multistate probability table and its corresponding SRCC. The SRCCs of wind speeds in the two WFs and their corresponding SRCCs of wind power outputs have been calculated and are shown in Table 1. It implies that when the wind speeds of the two WFs follow a certain correlation coefficient, the simulated wind power outputs should follow the corresponding Spearman correlation.

The multistate probability table of the two dependent WFs under different correlation coefficients of wind speeds (i.e., R$v$ equals 0.2, 0.5 and 0.9, respectively) is shown in Table 2. In our work, the fixed random number seeds are used to simulate wind speeds; thus, the state probabilities of WF_A remain unchanged, while the state probabilities of WF_B vary with wind speed correlation coefficients.

For convenience, the probabilistic distributions of output power of WF_B under different wind speed correlation are shown in Fig. 5. As depicted in Fig. 5, state probabilities of WF_B under different wind speed correlation coefficients are quite close. This indicates that the effect of wind speed correlation on sampling of wind farm outputs is mainly reflected on the correlation coefficients of wind farm outputs.

**Table 1**
Corresponding relation between SRCC of wind speeds and wind power outputs.

| | | | |
|---|---|---|---|
| SRCC of wind speeds | 0.2 | 0.5 | 0.9 |
| SRCC of wind power outputs | 0.1828 | 0.4622 | 0.8698 |

**Table 2**
State probability table of dependent WFs power outputs.

| Power outputs (MW) | State probabilities of WF_A and WF_B | | | |
|---|---|---|---|---|
| | WF_A | WF_B | | |
| | | R$v$ = 0.2 | R$v$ = 0.5 | R$v$ = 0.9 |
| 0 | 0.3293 | 0.3310 | 0.3313 | 0.3350 |
| 20 | 0.1120 | 0.1148 | 0.1130 | 0.1107 |
| 40 | 0.0893 | 0.0826 | 0.0876 | 0.0848 |
| 60 | 0.0697 | 0.0682 | 0.0678 | 0.0684 |
| 80 | 0.0557 | 0.0633 | 0.0575 | 0.0546 |
| 100 | 0.0472 | 0.0460 | 0.0463 | 0.0475 |
| 120 | 0.0407 | 0.0363 | 0.0397 | 0.0403 |
| 140 | 0.0315 | 0.0342 | 0.0342 | 0.0321 |
| 160 | 0.0303 | 0.0284 | 0.0270 | 0.0300 |
| 180 | 0.1063 | 0.1061 | 0.1063 | 0.1058 |
| 200 | 0.0882 | 0.0891 | 0.0894 | 0.0908 |

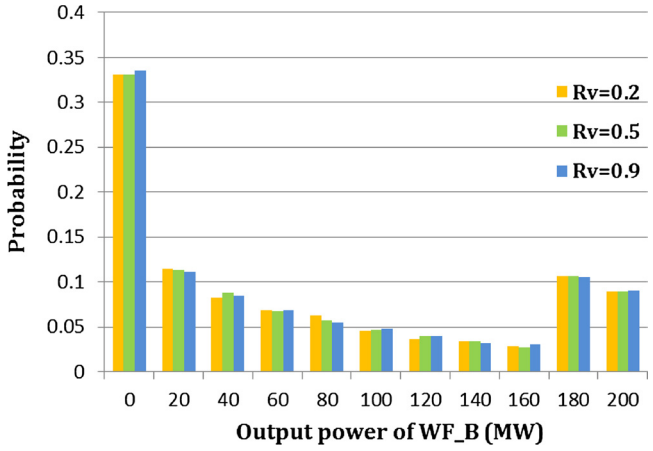


**Fig. 5.** Probabilistic distributions of WF_B under different wind speed correlation.

#### 4.2.2. Composite power system reliability evaluation of MRTS_A1

The correlation coefficient of wind speed series of the two WFs is set to be 0.5 in this section. To ensure accuracy in non-sequential MCS, the coefficient of variance is often used as the stopping rule in the sampling. It has been found that the coefficient of variance of EENS index has the lowest rate of convergence among many risk indices [2]. Therefore, the coefficient of variance for EENS index is used as the convergence criterion and is set to be 2% in our case study. By running program, it is found that the sampling number of non-sequential MCS is 93,359 when the convergence for EENS index (i.e., $\beta_{EENS} \leq 2\%$) is reached. Here, for the sake of comparison, the sample size of non-sequential MCS is set to be 100,000 in our case study (In fact, the $\beta_{EENS}$ corresponding with the sample size of 100,000 is 1.86%). To validate the effectiveness of the proposed accelerating techniques of the composite power system reliability evaluation, computation times of four computation scenarios are compared. The four computation scenarios are as follows:

- **Scenario 1**: neither the state merging technique nor the parallel computation technique is employed.
- **Scenario 2**: only the state merging technique is employed.
- **Scenario 3**: only the parallel computation technique is employed.
- **Scenario 4**: both the state merging technique and the parallel computation technique are employed.

**Table 3**
Comparison of evaluation efficiency of different cases for MRTS_A1.

| Scenarios | Thread number | *Nstates* | CPU time (s) | Time ratios |
|---|---|---|---|---|
| Scenario 1 | Single thread (Case 1) | 100,000 | 693 | 100% |
| Scenario 2 | Single thread (Case 2) | 28,555 | 316 | 45.60% |
| Scenario 3 | Two threads (Case 3) | 100,000 | 406 | 58.59% |
| | Four threads (Case 4) | 100,000 | 320 | 46.18% |
| Scenario 4 | Two threads (Case 5) | 28,555 | 189 | 27.27% |
| | Four threads (Case 6) | 28,555 | 153 | 22.08% |

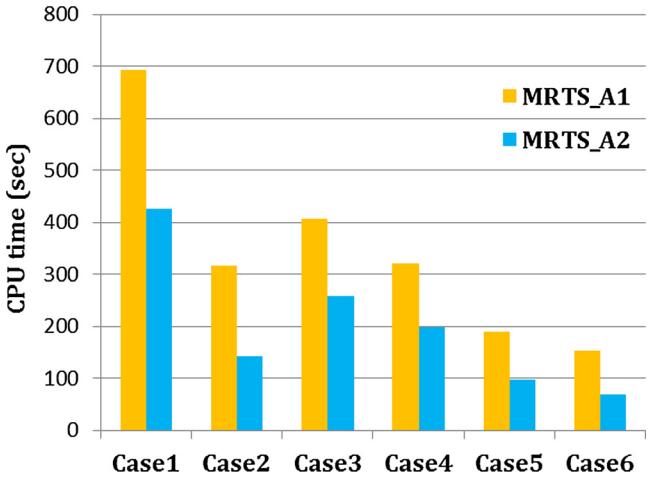


**Fig. 6.** CPU time in different computation cases.

In this paper, the program is performed on a personal computer with dual-core and four-threading configuration, and thus there are totally six computation cases for the reliability evaluation. The number of system states to be evaluated (designated as Nstates) of each computation case with its corresponding CPU time is shown in Table 3. Additionally, taking the CPU time in Case 1 as the benchmark, and the ratios of CPU times in the six cases to the CPU time in case 1 are given in the last column of Table 3. For the sake of comparison, the CPU time of MRTS_A1 in six computation cases is shown in Fig. 6 (also including CPU time of MRTS_A2). In the process of programming, the seeds for the random number generator in the six cases are set to be identical for the sake of comparison. Using the same random number seeds, reliability indices of MRTS_A1 in the six computation cases are the same. The probability of load curtailment (PLC) and the expected energy not supplied (EENS) are 0.04744 and 67362 (MWh/year), respectively.

As shown in Case 2 of Table 3, when the state merging technique is used, only 28.56% of the total system states have to be evaluated; thus, the computational time of the reliability assessment procedure in Case 2 is only 45.60% of the computational time in Case 1. This significant reduction verifies the effectiveness of the state merging technique. As shown in Table 3 and Fig. 6, when the parallel computation technique is applied, the computational times in Cases 3 and 4 are also greatly reduced compared to the computational time in Case 1. Moreover, in Case 3, it is worth noting that the computational time in two threads environment is 58.59% of the computational time in a single thread environment, which is larger than 50% of the time of serial computation. The reason lies in that it takes time to allocate task and communicate data among the processors when parallel computation technique is employed. In Case 4, it is also important to note that the computational time in four threads environment is 46.18% of the computational time in a single thread environment, which is less than 50% of the time of serial computation. The reason lies in that the hyper-threading technique refines parallel computation to thread level and implements dual thread parallel computing for a single processor. Owing to the hyper-threading technique, the computational ability of each computing unit of a single processor is fully utilized, further improving the computation efficiency of the CPU. Similarly, the CPU time in Case 6 is less than the CPU time in Case 5 owing to the utilization of hyper-threading technique. In general, it is significant that the computational time in Scenario 4 is the much less than the computational times in other scenarios, which demonstrates the validity of the proposed reliability evaluation algorithm integrated with state merging, parallel computation and hyper-threading techniques.

#### 4.2.3. Composite power system reliability evaluation of MRTS_A2

It is noted that under the constant sample size of system states, the higher the reliability of system components, the more likely to sample the same system states. In this context, we conclude that the state merging technique will be more effective for reliability evaluation of power system with high reliable components. To verify the deduction, we created a test system with high reliability components. First, we specially carried out statistical analysis on the reliability indices of the MRTS_A1 system. The statistical analysis showed that 97.47% of load curtailment is caused by failure events of generating units (the other 2.53% of load curtailment is caused by combination failure of generating units and transmission lines). Therefore, we reduce the FORs of MRTS_A1 conventional generating units by half to form the MRTS_A2 test system. The reliability indices of MRTS_A2 are obtained by running the reliability evaluation program, with the PLC is 0.01148 and the EENS is 13268 MWh/year, respectively. The computation efficiency information in the six computation cases for MRTS_A2 reliability evaluation is shown in Table 4. Especially, the CPU times of MRTS_A2 in six cases is also shown in Fig. 6, for the sake of comparison. As shown in Fig. 6, the CPU time of MRTS_A2 is less than that of MRTS_A1. The reason lies in that MRTS_A2 is a more reliable system and thus less contingency states need to be analyzed.

Moreover, comparing the computation results of Case 2 in Tables 3 and 4, we see that the total number of merged system states for MRTS_A2 (i.e., 13,330) is much less than the total number of merged system states for MRTS_A1 (i.e., 28,555), and correspondingly the time ratio of MRTS_A2 (i.e., 33.57%) is much less than that of MRTS_A1 (i.e., 45.60%). Technically, it implies that the computation improvement of the state merging technique is related to the reliability of system components: the higher the component reliability, the more significant the computation improvement of the state merging technique.

### 4.3. CC evaluation of WFs incorporating both wind power correlation and transmission constraints

The EENS is used as the reliability criterion to evaluate the CC of WFs in this paper. A series of numerical tests have been carried out to study the effects of some factors including wind speed correlation, transmission network constraints and WF-integrated locations on the CC of WFs. The evaluation results of different conditions will be listed in Tables 5–9 in the following sections. But now, for the convenience of comparison, the EELCs and CCs of WFs in Tables 5–9 are graphically shown in advance in Figs. 7 and 8.

#### 4.3.1. Effect of wind speed correlation

The MRTS_A1 system is used to investigate the effect of wind speed

**Table 4**
Comparison of evaluation efficiency of different cases for MRTS_A2.

| Scenarios | Thread number | *Nstates* | Run time (s) | Time ratios |
|---|---|---|---|---|
| Scenario 1 | Single thread (Case 1) | 100,000 | 426 | 100% |
| Scenario 2 | Single thread (Case 2) | 13,330 | 143 | 33.57% |
| Scenario 3 | Two threads (Case 3) | 100,000 | 259 | 60.80% |
| | Four threads (Case 4) | 100,000 | 197 | 46.24% |
| Scenario 4 | Two threads (Case 5) | 13,330 | 97 | 22.77% |
| | Four threads (Case 6) | 13,330 | 69 | 16.20% |

**Table 5**
The CC of WFs in MRTS_A1 (considering transmission constraints).

| Indices | Correlation coefficients of wind speeds | | |
|---|---|---|---|
| | 0.2 | 0.5 | 0.9 |
| ELCC (MW) | 112.50 | 106.25 | 96.88 |
| CC | 28.13% | 26.56% | 24.22% |

**Table 6**
The CC of WFs in MRTS_A1 (without considering transmission constraints).

| Indices | Correlation coefficients of wind speeds | | |
|---|---|---|---|
| | 0.2 | 0.5 | 0.9 |
| ELCC (MW) | 132.04 | 125.39 | 115.82 |
| CC | 33.01% | 31.35% | 28.96% |

**Table 7**
The CC of WFs in MRTS_A3 (considering transmission constraints).

| Indices | Correlation coefficients of wind speeds | | |
|---|---|---|---|
| | 0.2 | 0.5 | 0.9 |
| ELCC (MW) | 103.13 | 95.31 | 84.38 |
| CC | 25.78% | 23.83% | 21.09% |

**Table 8**
The CC of WFs in MRTS_B1 (considering transmission constraints).

| Indices | Correlation coefficients of wind speeds | | |
|---|---|---|---|
| | 0.2 | 0.5 | 0.9 |
| ELCC (MW) | 109.38 | 104.69 | 95.31 |
| CC | 27.35% | 26.17% | 23.83% |

**Table 9**
The CC of WFs in MRTS_B2 (considering transmission constraints).

| Indices | Correlation coefficients of wind speeds | | |
|---|---|---|---|
| | 0.2 | 0.5 | 0.9 |
| ELCC (MW) | 55.96 | 53.13 | 48.44 |
| CC | 13.99% | 13.28% | 12.11% |

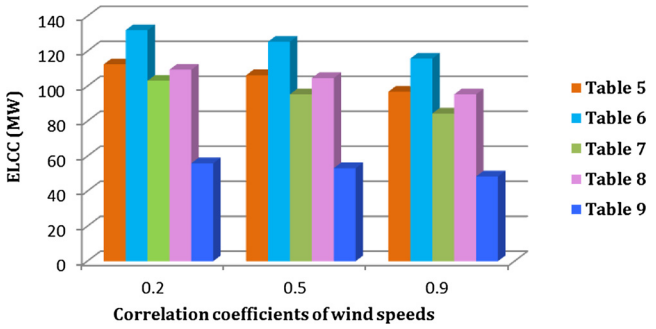


**Fig. 7.** ELCCs of WFs in different tables.

correlation on the CC of WFs in this section. Firstly, the EENS of the composite power system of IEEE RTS 79 is calculated and used as the benchmark of composite power system reliability. Then, the EENS of MRTS_A1 at different peak loads is calculated and compared with the EENS of IEEE RTS79 to obtain the ELCC of WFs. The ELCCs and CCs of WFs in MRTS_A1 with different wind speed correlation coefficients are

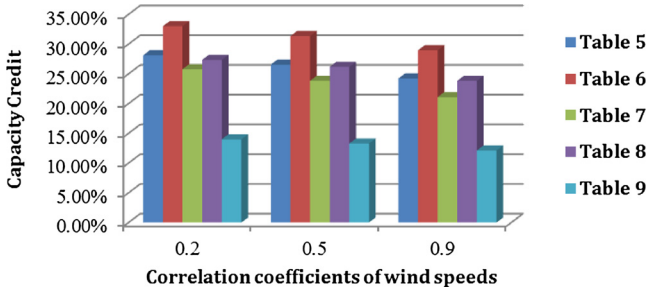


**Fig. 8.** The CCs of WFs in different tables.

shown in Table 5, while the transmission constraints are considered.

As shown in Table 5, the CC of WFs in MRTS_A1 decreases along with the increase of wind speed correlation coefficient. This is due to the fact that the wind speed correlation weakens the improvement effect of wind power on system reliability. Correspondingly, ELCC of WFs decreases under the equal reliability criterion. It can be concluded that the effect of wind speed correlation should be considered when evaluating the CC of multiple WFs, and the omission of wind speed correlation may lead to an optimistic result.

*4.3.2. Effect of transmission network constraints*

(1) The CC of WFs without considering transmission constraints

The CC of WFs considering only the stochastic failures of the generating system is calculated in this section to demonstrate the effect of transmission network constraints. Based on the generating system reliability assessment method, the EENS of the IEEE RTS79 generating system is calculated and used as the benchmark. Then the EELC of WFs in MRTS_A1 can be obtained by an iterative method. The ELCCs and CCs of WFs in MRTS_A1 without considering transmission network constraints are shown in Table 6.

As shown in Table 6, when the transmission line constraints are not considered, the CC of WFs in MRTS_A1 also decreases along with the increase of the wind speed correlation coefficient. Moreover, when we compare the results of EELC and CCs in Tables 5 and 6, it can be observed that the results in Table 5 are less than those in Table 6 (as shown in Figs. 7 and 8). This is because that the reliability improvement of WFs is weakened when transmission system outages and congestions are considered. The differences of results between Tables 5 and 6 suggest that it is essential to incorporate the transmission network constraints when evaluating the CC of WFs.

(2) Effect of transmission capacity limitations

As mentioned above, the MRTS_A1 test system has a strong transmission network but a weak generation system. In order to demonstrate the effect of transmission network on the CC of WFs, we create an MRTS_A3 system by reducing capacity limits of all transmission lines of the MRTS_A1 by half. The ELCCs and CCs of WFs in MRTS_A3 with different wind speed correlation coefficients are shown in Table 7.

Comparing the results in Tables 5–7 (as shown in Figs. 7 and 8), it is obvious that the ELCCs and CCs of WFs in Table 7 are the minimum and the ELCCs and CCs of WFs in Table 5 are the maximum. This not only validates the effect of transmission capacity constraints on the CC of WFs, but also shows the extent of effect of transmission constraints is related to the transmission capacity. The more adequate the transmission capacity is, the greater the CC of WFs.

(3) Effect of WFs integrated locations

To demonstrate the effect of WF locations on the CC of WFs, we try to change the integrated locations of MRTS_A1 WFs from buses 1 and 2 to buses 18 and 22, i.e., to construct a MRTS_B1 test system. The EELCs and CCs of MRTS_B1 WFs are calculated and shown in Table 8.

Comparing the results of MRTS_B1 in Table 8 with the results of MRTS_A1 in Table 5 (as shown in Figs. 7 and 8), it is observed that results in Table 8 are smaller than the results in Table 5. This suggests that the CC of WFs is related to the integrated locations of WFs. In fact,

the difference of CC of WFs between MRTS_A1 and MRTS_B1 is consistent with the network structure characteristics of IEEE RTS79. The north region of IEEE RTS79 is the area where considerable power sources are concentrated, while the south region of IEEE RTS79 is the area where considerable system loads are concentrated. A significant amount of power is therefore transferred from the northern to the southern part. When the WFs are integrated into IEEE RTS79 at buses 18 and 22 (i.e. MRTS_B1 test system), the line power flow from the north region to the south region will become heavier; thus, the reliability improvement of wind power injection will be reduced due to the line power flow constraints. When the WFs are integrated into IEEE RTS79 at buses 1 and 2 (i.e. MRTS_A1 test system), the heavy power flow from the north to south will be alleviated. Subsequently, higher reliability improvement of wind power can be obtained. This explains why the ELCCs of WFs are smaller when wind power is injected at buses 18 and 22, compared to when wind power is injected at buses 1 and 2.

On the other hand, it is also observed that the differences of results in Tables 5 and 8 are small (as also shown in Figs. 7 and 8), which indicates that the integrated location has relatively minor impact on the CC of WFs as for the IEEE RTS79 system. This is due to the fact that the IEEE RTS79 system has a strong transmission network. Though WFs are connected at different buses of IEEE RTS79, the injected wind power can be transferred to load points basically without congestion. To verify that the CC impact of connecting WFs at different locations is related to transmission system adequacy, we constructed a test gird with a weak transmission system. In this context, the capacity limits of all transmission lines of IEEE RTS79 are reduced by half. Then WFs are connected into the system at different buses to form MRTS_A3 and MRTS_B2 test systems. The CCs of WFs of MRTS_A3 are shown in Table 7, and the CCs of WFs of MRTS_B2 are then calculated and shown in Table 9.

Comparing the results of MRTS_A3 in Table 7 with results of MRTS_B2 in Table 9 (as shown in Figs. 7 and 8), it can be observed that results in Table 9 are smaller than the results in Table 7 and the differences of results in Tables 7 and 9 are significant. This indicates that the integrated locations have great impact on the CC of WFs, as well as for the modified test system with weak transmission network. In fact, the observation is consistent with the topology and operating conditions of MRTS_A3 and MRTS_B2 systems. The capacity ratings of all transmission lines of MRTS_A3 and MRTS_B2 are only half of the original IEEE RTS 79, so there is considerable utilization of the transmission network in these two systems when they are considered to be under stress. As for the MRTS_A3 system, the WFs are connected at a load area (buses 1 and 2), therefore the transmission congestion is alleviated and the CC of WFs is relatively high. In contrast, as for the MRTS_B2 system, the WFs are connected at a power source area (buses 18 and 22), therefore the transmission congestion worsens and the injected wind power cannot fully be distributed to the load points, and finally lead to a lower CC.

Moreover, it can be observed that in Table 9, the differences of the EELCs and CCs under different wind speed correlation coefficients are small, which implies that wind speed correlation has relatively minor impact on the CC of WFs. The reason for this is that the impact of wind speed correlation is swamped by the impact of transmission network congestion of MRTS_B2 system.

## 5. Conclusion

A non-sequential MCS based reliability assessment method of composite power system with dependent wind farms is proposed in this paper. First of all, the WFs outputs are proposed to be modeled by combining the multistate probability table with SRCCs. In this way, the outputs of WFs can be appropriately simulated by using dependent random variables under the non-sequential MCS frame. Subsequently, a special array is constructed to represent each system state simulated by non-sequential MCS and then this array is represented by a decimal number, which facilitates the merging of the entire simulated system states. And as for the merged system states, parallel computing technique is used for their contingency analysis. Furthermore, based on the proposed composite power system reliability assessment algorithm, a computing framework for the CC evaluation of WFs considering both wind power correlation and transmission network constraints is proposed. Numerical results on five test systems validate the effectiveness of the proposed reliability assessment method and the necessity of considering wind speed correlation and transmission constraints in the CC evaluation. In addition, there are some meaningful conclusions about the CC evaluation of WFs worth to be pointed out, as follows:

(1) The impact of wind speed correlation on the CC of WFs is related to the transmission congestion level and the locations of WFs. As for a power system with strong transmission, the impact of wind speed correlation is relatively considerable. While as for a power system with weak transmission, the impact of wind speed correlation is further dependent on the locations used to connect WFs. If WFs are connected in the power source area, then the reliability improvement of wind power may be swamped due to transmission system outages and congestions, leaving the differences of CC among different wind speed correlation coefficients small. Conversely, if WFs are connected in the load area, then the wind power can be successfully transmitted into load points. As a result, the impact of wind speed correlation will be relatively obvious.
(2) Similarly, the impact of integrated locations of WFs on the CC of WFs is related to the transmission congestion level. As for a power system with heavy transmission burden, there is great impact on the CC; while as for a power system with adequate transmission capability margin, the impact is slight.

Different from existing works focusing on improving the sampling efficiency of system states [7–10], we focus on dealing with system states which are simulated by non-sequential MCS to accelerate the reliability evaluation of composite power system. However, it should be pointed out that our proposed method is compatible with these advanced sampling methods. In addition, the frequency and duration (F&D) indices are important in practical application of composite power system reliability assessment. A lot of studies have been conducted on calculating F&D by non-sequential MCS or its improved methods [4–6,9,30,31]. The proposed method of this paper is under the frame of non-sequential MCS, thus it is potential to calculate the F&D indices of composite power system with WFs. Our future work includes integrating the proposed accelerating method with the existing advanced sampling methods to improve the computational efficiency, and calculating the F&D induces.

## Acknowledgements

The authors are grateful for the support from the Open Research Fund of Jiangsu Collaborative Innovation Center for Smart Distribution Network (No. XTCX201612) and the Scientific Research Fund of Nanjing Institute of Technology in China (No. ZKJ201607).

## References

[1] R. Billinton, W. Li, Reliability Assessment of Electric Power Systems Using Monte Carlo Method, Plenum Press, New York, USA, 1994.
[2] W. Li, Risk Assessment of Power Systems: Models, Methods, and Applications, 2nd ed., Wiley-IEEE Press, New Jersey, USA, 2014.
[3] A.M. Leite Da Silva, J.F. Costa Castro, R.A. Gonzalez-Fernandez, Spinning reserve assessment under transmission constraints based on cross-entropy method, IEEE Trans. Power Syst. 31 (March) (2016) 1624–1632.
[4] A.M. Leite Da Silva, X. Gonza, X. Lez-Ferna, R.A. Ndez, W.S. Sales, L.A.F. Manso, Reliability assessment of time-dependent systems via quasi-sequential Monte Carlo simulation, 11th International Conference on Probabilistic Methods Applied to Power Systems (PMAPS) (2010) 697–702.
[5] J.C.O. Mello, M.V.F. Pereira, A.M.L.D. Silva, Evaluation of reliability worth in

composite systems based on pseudo-sequential Monte Carlo simulation, IEEE Trans. Power Syst. 9 (August (3)) (1994) 1318–1326.
[6] A.M. Leite Da Silva, L.A. Da Fonseca Manso, J.C. De Oliveira Mello, R. Billinton, Pseudo-chronological simulation for composite reliability analysis with time varying loads, IEEE Trans. Power Syst. 15 (February (1)) (2000) 73–80.
[7] C. Hamon, M. Perninge, L. Söder, An importance sampling technique for probabilistic security assessment in power systems with large amounts of wind power, Electr. Power Syst. Res. 131 (February) (2016) 11–18.
[8] Z. Shu, P. Jirutitijaroen, A.M. Leite Da Silva, C. Singh, Accelerated state evaluation and Latin hypercube sequential sampling for composite system reliability assessment, IEEE Trans. Power Syst. 29 (January (4)) (2014) 1692–1700.
[9] R.A. Gonzalez-Fernandez, A.M. Leite Da Silva, L.C. Resende, M.T. Schilling, Composite systems reliability evaluation based on Monte Carlo simulation and cross-entropy methods, IEEE Trans. Power Syst. 28 (November (4)) (2013) 4598–4606.
[10] B. Hua, Z. Bie, S. Au, W. Li, X. Wang, Extracting rare failure events in composite system reliability evaluation via subset simulation, IEEE Trans. Power Syst. 30 (March (2)) (2015) 753–762.
[11] W. Wangdee, R. Billinton, Probing the intermittent energy resource contributions from generation adequacy and security perspectives, IEEE Trans. Power Syst. 27 (November (4)) (2012) 2306–2313.
[12] Z. Ning, K. Chongqing, D.S. Kirschen, X. Qing, Rigorous model for evaluating wind power capacity credit, IET Renew. Power Gener. 7 (August (5)) (2013) 504–513.
[13] E. Gil, I. Aravena, Evaluating the capacity value of wind power considering transmission and operational constraints, Energy Convers. Manage. 78 (February) (2014) 948–955.
[14] Y. Guo, H. Gao, Q. Wu, A combined reliability model of VSC-HVDC connected offshore wind farms considering wind speed correlation, IEEE Trans. Sustain. Energy 8 (October (4)) (2017) 1637–1646.
[15] S.M. Miryousefi Aval, A. Ahadi, H. Hayati, A novel method for reliability and risk evaluation of wind energy conversion systems considering wind speed correlation, Front. Energy 10 (March (1)) (2016) 46–56.
[16] A. Ghaedi, A. Abbaspour, M. Fotuhi-Firuzabad, M. Moeini-Aghtaie, Toward a comprehensive model of large-scale DFIG-based wind farms in adequacy assessment of power systems, IEEE Trans. Sustain. Energy 5 (August (1)) (2014) 55–63.
[17] F. Chen, F. Li, Z. Wei, G. Sun, J. Li, Reliability models of wind farms considering wind speed correlation and WTG outage, Electr. Power Syst. Res. 119 (February) (2015) 385–392.
[18] G. Díaz, P.G. Casielles, J. Coto, Simulation of spatially correlated wind power in small geographic areas—sampling methods and evaluation, Int. J. Electr. Power Energy Syst. 63 (December) (2014) 513–522.
[19] D. Cai, D. Shi, J. Chen, Probabilistic load flow computation using Copula and Latin hypercube sampling, IET Gener. Transm. Distrib. 8 (September (9)) (2014) 1539–1549.
[20] X. Xu, Z. Yan, Probabilistic load flow evaluation considering correlated input random variables, Int. Trans. Electr. Energy Syst. 26 (May) (2016) 555–572.
[21] S.M. Mousavi Agah, D. Flynn, Impact of modelling non-normality and stochastic dependence of variables on operating reserve determination of power systems with high penetration of wind power, Int. J. Electr. Power Energy Syst. 97 (April) (2018) 146–154.
[22] J. Xu, P.K. Kanyingi, K. Wang, G. Li, B. Han, X. Jiang, Probabilistic small signal stability analysis with large scale integration of wind power considering dependence, Renew. Sustain. Energy Rev. 69 (March) (2017) 1258–1270.
[23] G. Papaefthymiou, D. Kurowicka, Using copulas for modeling stochastic dependence in power system uncertainty analysis, IEEE Trans. Power Syst. 24 (February (1)) (2009) 40–49.
[24] R.S. Kumar, E. Chandrasekharan, A parallel distributed computing framework for Newton-Raphson load flow analysis of large interconnected power systems, Int. J. Electr. Power Energy Syst. 73 (December) (2015) 1–6.
[25] S. Varshney, L. Srivastava, M. Pandit, A parallel computing approach for integrated security assessment of power system, Int. J. Electr. Power Energy Syst. 78 (June) (2016) 591–599.
[26] J.A. Martinez, G. Guerra, A parallel Monte Carlo method for optimum allocation of distributed generation, IEEE Trans. Power Syst. 29 (November (6)) (2014) 2926–2933.
[27] L. Garver, Effective load carrying capability of generating units, IEEE Trans. Power Apparatus Syst. 85 (August (8)) (1966) 910–919.
[28] C.J. Dent, A. Hernandez-Ortiz, S.R. Blake, D. Miller, D. Roberts, Defining and evaluating the capacity value of distributed generation, IEEE Trans. Power Syst. 30 (September (5)) (2015) 2329–2337.
[29] IEEE Committee Report, IEEE reliability test system, IEEE Trans. Power Apparatus Syst. PAS-98 (November (6)) (1979) 2047–2054.
[30] A.C.G. Melo, M.V.F. Pereira, A.M. Leite Da Silva, Frequency and duration calculations in composite generation and transmission reliability evaluation, IEEE Trans. Power Syst. 7 (May (2)) (1992) 469–476.
[31] A.C.G. Melo, M.V.F. Pereira, A.M. Leite Da Silva, A conditional probability approach to the calculation of frequency and duration indices in composite reliability evaluation, IEEE Trans. Power Syst. 8 (August (3)) (1993) 1118–1125.